Systematic development of peptide inhibitors targeting the CXCL12/HMGB1 interaction

Jacopo Sgrignani[a,§], Valentina Cecchinato[a,§], Enrico M.A. Fassi[a,b,§], Gianluca D'Agostino[a], Maura Garofalo[a], Gabriela Danelon[a], Mattia Pedotti[a,], Luca Simonelli[a], Luca Varani[a,], Giovanni Grazioso[b], Mariagrazia Uguccioni[a,c◆*] and Andrea Cavalli[a,d◆*]

[a]Institute for Research in Biomedicine, Università della Svizzera italiana, CH-6500 Bellinzona, Switzerland

[b] Dipartimento di Scienze Farmaceutiche, Università degli Studi di Milano, 20133, Milan, Italy.

[c]Department of Biomedical Sciences, Humanitas University, 20090 Pieve Emanuele – Milan, Italy

[d]Swiss Institute of Bioinformatics, 1015 Lausanne, Switzerland

§: these authors contributed equally to this work
◆: these authors contributed equally to this work
* Corresponding authors

Abstract

During inflammatory reactions, the production and release of chemotactic factors guide the recruitment of selective leukocyte subpopulations. The alarmin HMGB1 and the chemokine CXCL12, both released in the microenvironment, can form a heterocomplex, which exclusively acts on the chemokine receptor CXCR4, enhancing cell migration and, in some pathological conditions such as Rheumatoid Arthritis exacerbates the immune response. An excessive cell influx at the inflammatory site can be diminished by disrupting the heterocomplex.

Here, we report the computationally driven identification of the first peptide (HBP08) binding HMGB1 and selectively inhibiting the activity of the CXCL12/HMGB1 heterocomplex. Furthermore, HBP08 binds HMGB1 with the highest affinity reported so far (K_d of 0.8 ± 0.4 μM). The identification of this peptide represents an important step towards the development of innovative pharmacological tools for the treatment of severe chronic inflammatory conditions characterized by an uncontrolled immune response.

Keywords

Peptide inhibitors, computational drug design, cell migration, inflammation, HMGB1, CXCL12, CXCL12/HMGB1 heterocomplex

Introduction

Chemokines are key regulators of leukocyte migration and play fundamental roles both in physiological and pathological immune responses.[1] Chemokine receptors, differentially expressed by all leukocytes and many non-hematopoietic cells, including cancer cells, constitute the largest branch of the γ subfamily of rhodopsin-like G-protein-coupled receptors (GPCR). In modern pharmacology, this receptor superfamily represents the most successful target of small molecule inhibitors to treat a variety of human diseases.[2] In the last 25/30 years, an impressive amount of preclinical and clinical evidence has progressively validated the role of chemokines and their receptors in immune-mediated diseases.[3, 4]

In the last decade, several studies have pointed out how the influence of chemokines on cell migration can be modulated by their binding to other chemokines or proteins released in inflammation.[5, 6] In particular, our group has shown that High Mobility Group Box1 (HMGB1), an alarmin released under stress conditions, forms a heterocomplex with the chemokine CXCL12, favoring cell migration *via* the activation of the chemokine receptor CXCR4 in the presence of a concentration of CXCL12, which normally does not trigger a cellular response.[7] In mammalian cells, HMGB1 is a highly conserved non-histone nuclear protein, which acts as a DNA chaperon, contributing to gene transcription and DNA repair.[8] Structurally, it is composed of two homologous, but not identical domains, BoxA and BoxB, and a negatively charged C-terminal tail (Figure 1).[9] Besides its nuclear function, HMGB1 is passively released by necrotic cells or actively released under inflammatory conditions and acts as an alarmin.[10, 11]

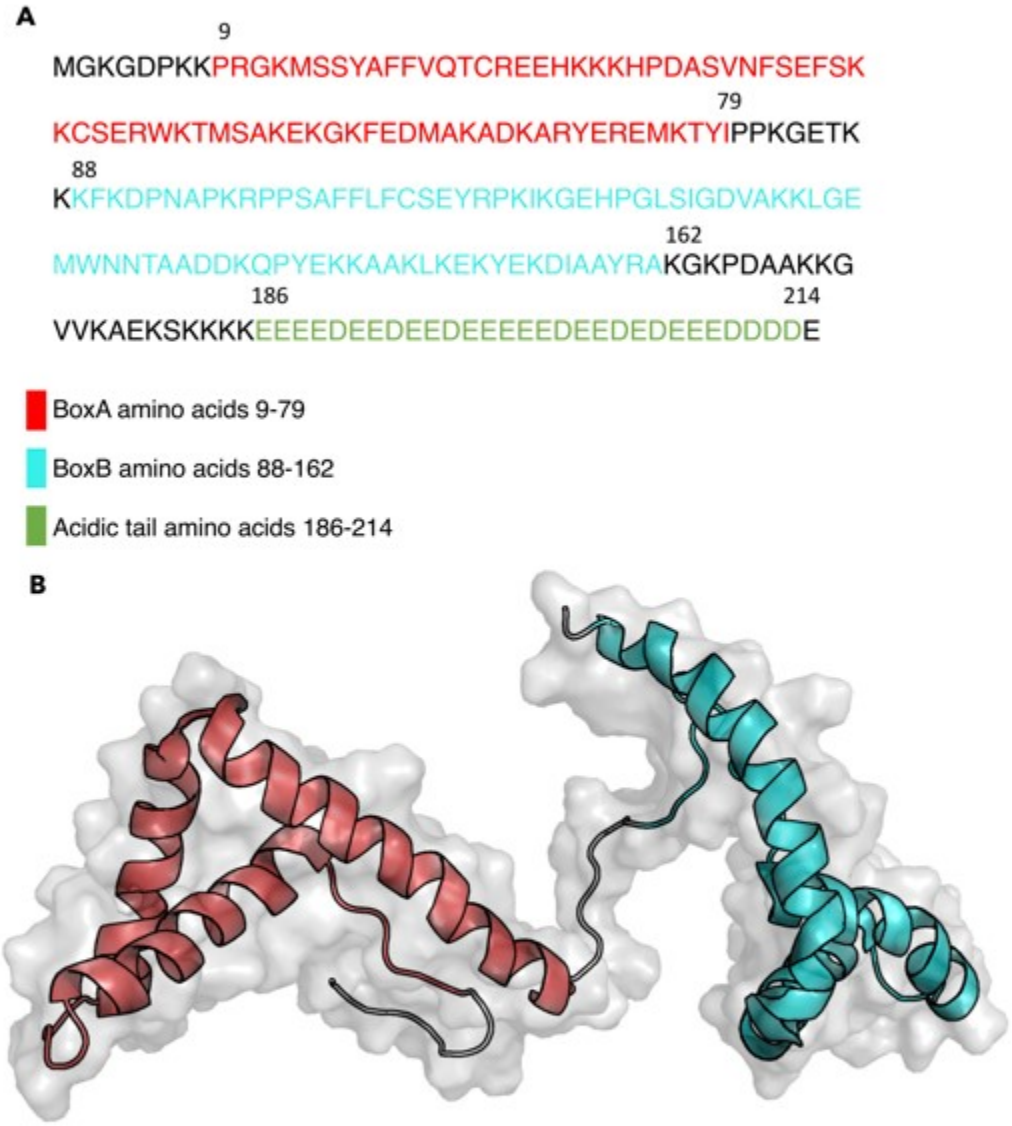

Figure 1. HMGB1 sequence and structure. (**A**) Amino acid sequence of HMGB1. Residues constituting the two boxes are shown in red (BoxA) and cyan (BoxB), while the acidic tail is

shown in green. (**B**) Ribbon representation of the two boxes of HMGB1 structure in solution (fragment 2-174, PDB code 2YRQ).

In the extracellular space, HMGB1 can be found in different redox states, depending on the presence of an intramolecular disulfide bond between two cysteines at positions 23 and 45.[12] Reduced HMGB1, in the extracellular space, can form a heterocomplex with CXCL12 and synergistically promote, via CXCR4, the recruitment of leukocytes to inflammatory sites.[7, 13, 14] Moreover, reduced HMGB1 can bind to the receptor for advanced glycation endproducts (RAGE) to induce CXCL12 secretion and autophagy.[15] Once oxidized by reactive oxidative species present in the extracellular space, HMGB1 binds to the Toll-like Receptor 4 (TLR4) leading to activation of the nuclear factor kappa-B (NF-kB) and transcription of cytokines, and chemokines.[12, 16]

Recently, we demonstrated that the CXCL12/HMGB1 heterocomplex is present in the synovial fluid of patients affected by Rheumatoid Arthritis (RA), and that its function is maintained in patients with active disease.[13] These findings indicate a crucial role of the CXCL12/HMGB1 heterocomplex in the recruitment of immune cells at sites of joint inflammation and to its contribution to the perpetuation of the chronic inflammation observed in RA.[13] Moreover, Pitzalis and coworkers have recently pointed out that the composition of the synovial tissue of patients with RA is strictly related with the response to therapies.[17] Several therapeutic approaches based on the use of biological and synthetic therapies are currently in use to treat RA, but a portion of patients does not benefit from the treatments, and only 20-30% of them reach a low disease activity status.[17, 18]

Therefore, small molecules or peptides able to hinder the formation of this heterocomplex could be useful as novel personalized therapeutic strategies.

To date, despite the importance of this target, only a few inhibitors of the CXCL12/HMGB1 interaction, or of the HMGB1 functions have been identified.[19-22] Currently, glycyrrhizin is the most potent and the best structurally characterized inhibitor of the CXCL12/HMGB1 heterocomplex but has a low affinity for HMGB1 (K_d ~ 150 μM), and it lacks specificity.[7, 19, 22]

In a recent review, Nuss and coworkers pointed out how peptides are still largely unconsidered when a drug discovery campaign starts[23] and summarize the reasons for this in three points: (1) peptides are the natural biological messengers for most endocrine signaling pathways, (2) peptides are membrane-impermeable and (3) peptides are biologically unstable. However, recent efforts have been successful in the development of innovative strategies to overcome these intrinsic limitations improving bioavailability and metabolic stability.[24-26] For this reason and because of their ability in targeting large surfaces as those involved in protein-protein interactions, peptides are receiving increasing attention.[27,22] It is estimated that over 400 peptides are in clinical development, and 60 are already available for therapeutic use in different countries.[28, 29]

Motivated by these observations, we applied computational chemistry techniques to develop a novel high-affinity nonapeptide able to inhibit the formation of the CXCL12/HMGB1 heterocomplex and to abolish the synergistic effect on cell migration in CXCR4 transfected cells and human monocytes, without affecting the ability of HMGB1 to trigger TLR4. The identified peptide, HBP08, is the strongest HMGB1 binder reported so far, with an affinity Kd of 0.8 μM.

Results and Discussion

Design of a peptide inhibitor of the CXCL12/HMGB1 interaction

Taking advantage of the known interaction between glycyrrhizin and HMGB1,[19] we applied a computational pipeline to identify selective peptide inhibitors of the CXCL12/HMGB1 interaction (Figure 2A).

We generated a model of the glycyrrhizin/BoxA complex consistent with the results of previously reported NMR chemical shift perturbation studies (Figure 2B).[19] In particular, in the generated model, glycyrrhizin interacts with Gln20 and Arg23 and occupies the region at the junction of the two arms of L-shape that characterizes the two HMGB1 boxes.

To maximize the heterogeneity of the peptides considered in our screening, we generated a library of 40.000 nonapeptides with a randomly selected sequence. All peptides were docked in the glycyrrhizin binding site and ranked according to the binding energy (Figure 2C, See Materials and Methods). Finally, aiming to reduce the number of potential false positives, the best 100 ranking peptides were re-docked to BoxA, using the peptide docking protocol of the program Glide[30] in an 'unbiased way', i.e. leaving the algorithm free to search for the best binding site on the protein surface.

The peptides resulting after these calculations were visually inspected and only the best GSCORE (a scoring function aimed to estimate binding affinity) pose of 57 peptides with a glycyrrhizin-like binding mode were retained for further analysis (Table S1).

Several studies have shown that approximated free energy methods like MM-GBSA,[31, 32] especially when coupled with long MD simulations, can be a valuable help in the selection of active peptides in virtual screening investigations.[33-35] Therefore, a 500 ns long MD simulation was performed for each of the 57 peptides obtained from docking calculations. Those detaching from the BoxA binding pocket during the simulations (14 out of 57) were considered unstable and not further analyzed in MM-GBSA calculations (Table S1).

Based on the MM-GBSA score, 13 different peptides were selected to be tested *in vitro* (Table 1, and Figure S1).

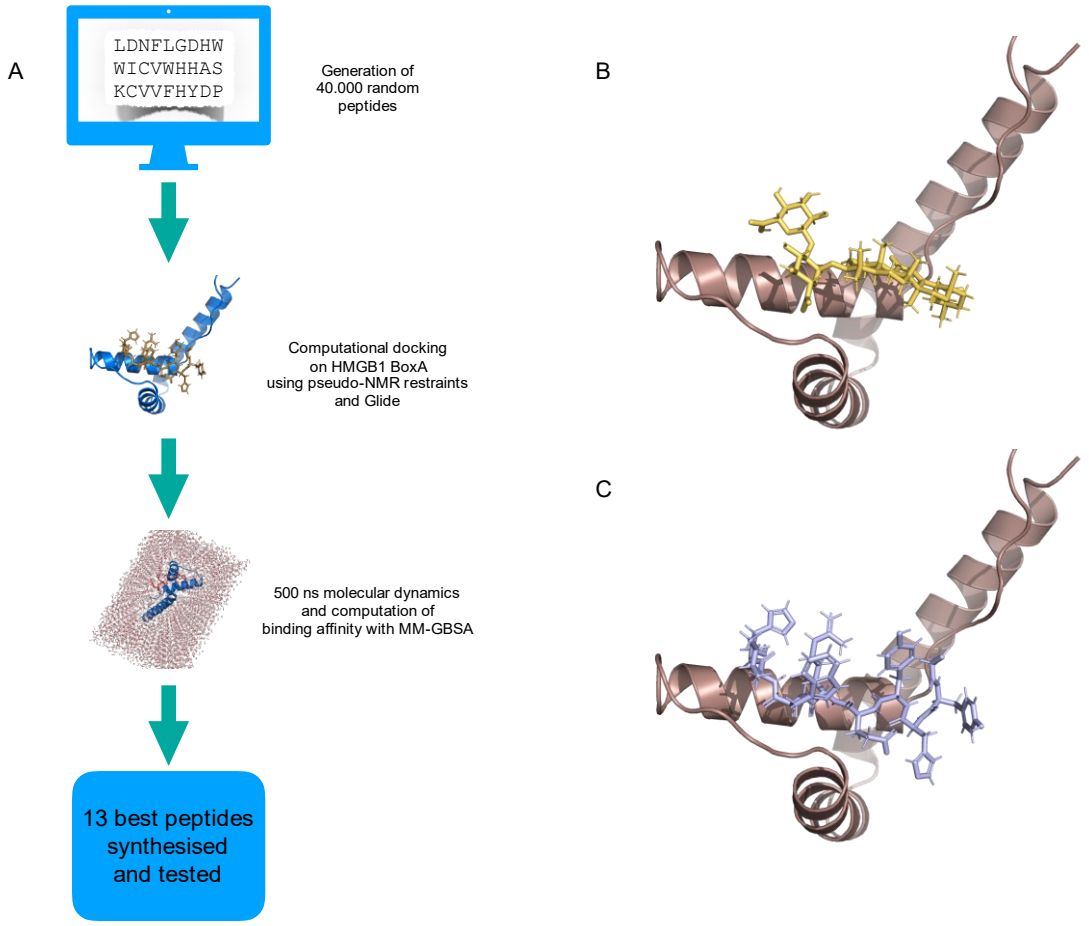

Figure 2. Computational strategy. (**A**) Workflow diagram of the computational pipeline used for the identification of the binding peptides. Peptides with a randomly generated sequence were first docked using pseudo-NMR restraints and then re-docked with Glide. Finally, peptides were ranked according to their binding free energy (ΔG) computed using MMGBSA with explicit water simulations of 500ns. (**B**) Model of the glycyrrhizin-BoxA complex used to define the peptide binding site. (**C**) Model of the complex of one of the identified peptides (HBP08) with BoxA obtained after the first docking

Table 1. List of binding peptides ranked according to their theoretical binging free energy ΔG.

Peptide Code	Sequence	ΔG_{GB}±SE [kcal/mol]
HBP01	HEMYWEDEW	-52.8±0.3
HBP02	IDLRFFMRQ	-52.0±0.3
HBP03	FAFELIQTD	-51.7±0.4
HBP04	CIPMMMHAW	-50.0±0.3
HBP05	WISNWILMW	-45.8±0.3
HBP06	TWNIHFADH	-45.6±0.4
HBP07	HWTLANWCR	-45.2±0.4
HBP08	GYHYERWIH	-45.1±0.5
HBP09	QFMKNCEEM	-44.8±0.4
HBP10	SINWHMYVN	-44.8±0.3
HBP11	MYRENQPTR	-42.9±0.4
HBP12	YHICWYGDY	-42.5±0.5
HBP13	WLWYEWGWQ	-41.9±0.3

In vitro assessment of the identified peptides.

The 13 identified peptides were tested in *in vitro* chemotaxis assay on a murine cell line expressing the human CXCR4 to evaluate their efficacy as inhibitors of the CXCL12/HMGB1-induced migration. Our experiments showed that 4 out of 13 peptides efficaciously inhibited the enhanced migration induced by the CXCL12/HMGB1 heterocomplex (Figure 3A). Of note, the inhibition observed using 100 μM of HBP05, HBP07, HBP08, or HBP12 was similar or better than the one observed using glycyrrhizin at 200 μM (Figure 3A). Further experiments performed with CXCL12 alone, showed that HBP07 and HBP08 do not affect CXCL12-induced cell migration, while HBP05 and HBP12 inhibit the migration induced by the chemokine alone (Figure 3B), therefore they were not used for further experiments. HBP07 and HBP08 were then tested on primary human monocytes. Only the HBP08 significantly blocked the activity of the heterocomplex (Figure 3C), without altering the migration induced by CXCL12 alone (Figure 3D), and exhibited no toxicity on both cell types (Figure S2). A

dose-response curve of the migration induced by the heterocomplex in the presence of scaling concentrations of the HBP08 peptide revealed that 50% of inhibition can be observed at 50 µM of the HBP08 peptide (Figure 3E).

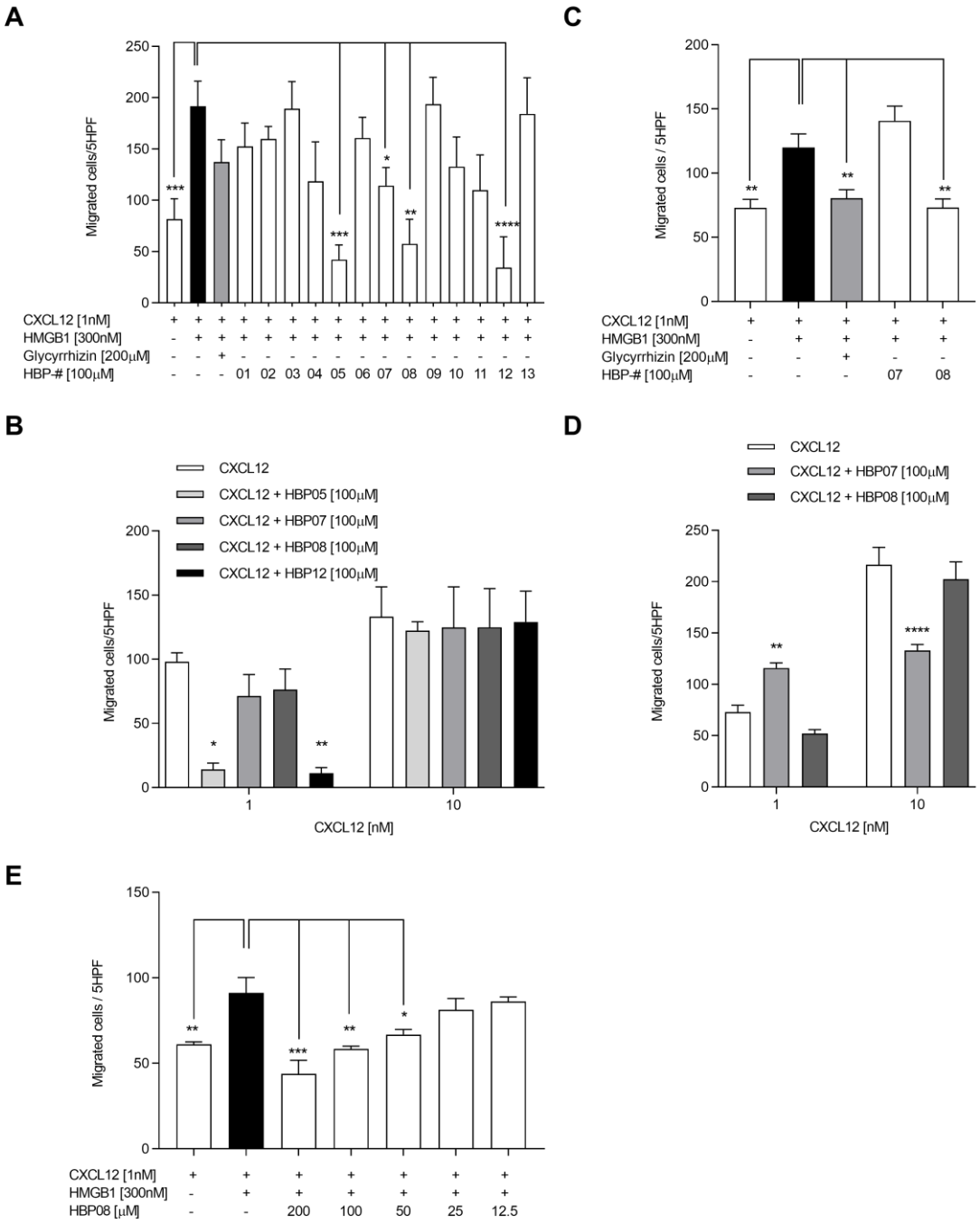

Figure 3. *In vitro* activity of the identified peptides. (**A**) Inhibition of cell migration in response to the CXCL12/HMGB1 heterocomplex was assessed on 300-19 Pre-B cells transfected with human CXCR4 using the identified peptides or glycyrrhizin. The numbers in the last horizontal row correspond to the different peptides. (**B**) Migration induced on 300-19 Pre-B cells transfected with CXCR4 by CXCL12 alone in the presence or absence of the peptides identified in (A) as inhibitors of the migration induced by the heterocomplex. (**C**) Inhibition of cell migration in response to the CXCL12/HMGB1 heterocomplex was assessed on human monocytes using HBP07, HBP08, or glycyrrhizin. (**D**) Migration induced on monocytes by CXCL12 alone in the presence or absence of HBP07, HBP08. (**E**) Inhibition of cell migration in response to the CXCL12/HMGB1 heterocomplex was assessed on 300-19 Pre-B cells transfected with CXCR4 using scaling concentrations of HBP08. (A-E) Migrated cells were counted in 5 high-power fields (HPF), and data are shown as mean±SEM of at least three independent experiments performed. *p<0.05; **p<0.01; ***p<0.001; ****p<0.0001 by one-way ANOVA followed by Dunnett's multicomparisons test (A, C, E), or two-way ANOVA followed by Tukey's multicomparisons test (B, D).

Selective activity of the HBP08 peptide

In the extracellular space oxidized HMGB1, through the binding to TLR4, activates the NF-kB pathway, and induces the transcription of several pro-inflammatory cytokines.[12, 16] In order to determine whether HBP08 was a selective inhibitor of the activity of the CXCL12/HMGB1 heterocomplex or could also prevent the binding of HMGB1 to its receptor TLR4, we performed a cytokine release assay on monocytes treated with HMGB1 alone, or in the presence of HBP08. We observed a significant release of IL-6 and TNF, which could be blocked by the treatment with a neutralizing antibody against TLR4 (Figure 4A, B). The peptide did not induce IL-6 or TNF release and did not block the HMGB1-mediated release of

these cytokines. These data indicate that HBP08 selectively inhibits the CXCL12/HMGB1 heterocomplex activity, leaving HMGB1 able to trigger TLR4.

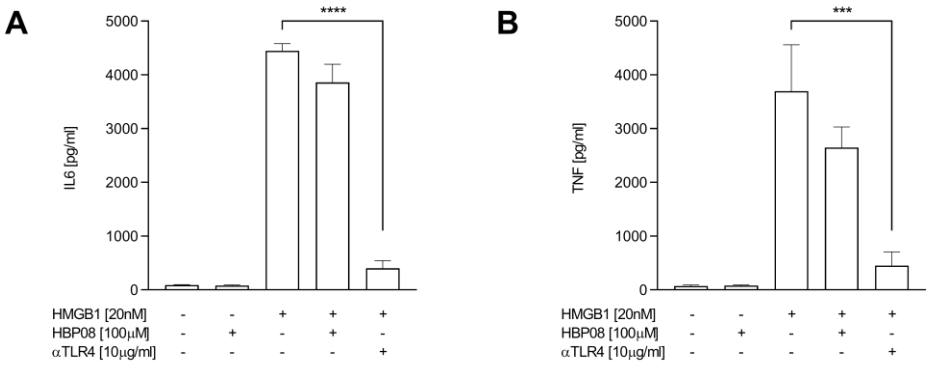

Figure 4. HMGB1-induced release of IL-6 and TNF via TLR4 is not inhibited by HBP08. The concentration of IL-6 (**A**) and TNF (**B**) in the supernatant of monocytes treated with HMGB1 in the presence of HBP08 or a neutralizing antibody against TLR4 (αTLR4) was measured by CBA. Data are shown as mean±SEM of at least four independent experiments performed. ***p<0.001; ****p<0.0001 by one-way ANOVA followed by Dunnett's multicomparisons test.

Characterization of the HMGB1-HBP08 interaction

Microscale thermophoresis (MST) was performed to determine the affinity of HBP08 to HMGB1, resulting in a K_d of 0.8 ± 0.4 μM (Figure 5). The affinity for HMGB1 of the identified peptide is, therefore, orders of magnitude higher than the other molecules reported in the literature so far, glycyrrhizin (K_d ~ 150 μM), diflunisal (K_d ~ 1.6mM) and mM 5,5-methylenedi-2,3-cresotic acid (K_d ~ 0.9mM).[19] Overall, these results indicate HBP08 as the inhibitor of the CXCL12/HMGB1 heterocomplex with the highest affinity for HMGB1.

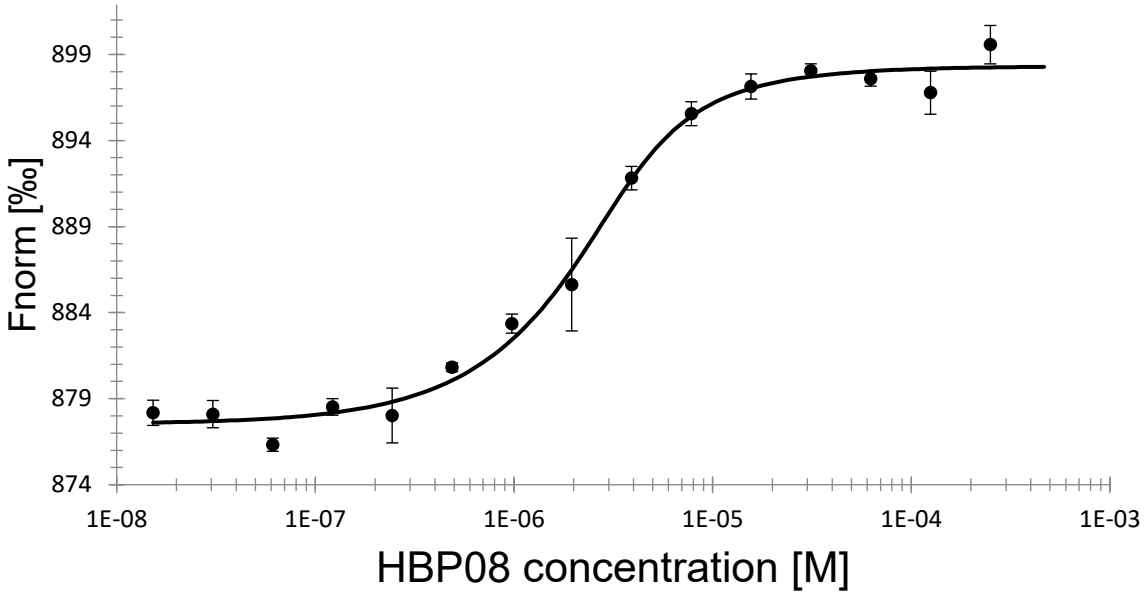

Figure 5. Microscale thermophoresis analysis of the interaction between HBP08 and HMGB1 (K_d = 0.8 ± 0.4 μM). The first point of the titration (500 μM) was an outlier with respect the titration curve suggesting that another binding event could be observed at very high peptide concentration, therefore, it was excluded by the fitting,

Given the structure of the target, which is composed of two highly homologous boxes, BoxA and BoxB, a 1:1 or 1:2 stoichiometry of the HMGB1/HPB08 complex with a peptide bound to BoxA and/or to BoxB, are both theoretically possible.

To clarify this point, we performed MST experiments with the two constructs containing only BoxA and BoxB, respectively. Interestingly, these experiments showed that HBP08 binds BoxA with the same affinity as for the full-length protein (Kd = 0.8 ± 0.3 μM, Figure S3,) while the affinity for BoxB is slightly lower (Kd = 17 ± 3.8 μM, Figure S4). Therefore, we can reasonably assume that, at the concentration used in migration experiments, an HMGB1/(HBP08)2 complex is present.

Moreover, to identify the most important residues for the binding, we performed a systematic alanine scanning of HBP08 (Table 2).

Table 2. Equilibrium dissociation constant (K_d) for the complexes between HMGB1 and the peptide of the first column.

Peptide name	Peptide sequence	K_d (μM)
HBP08	GYHYERWIH	0.8 ± 0.4
HBP08-Ala1	AYHYERWIH	8.6 ± 3.5
HBP08-Ala2	GAHYERWIH	5.8 ± 1.1
HBP08-Ala3	GYAYERWIH	26.2 ± 4.8
HBP08-Ala4	GYHAERWIH	9.9 ± 1.3
HBP08-Ala5	GYHYARWIH	0.8 ± 0.2
HBP08-Ala6	GYHYEAWIH	N.D. #
HBP08-Ala7	GYHYERAIH	22.0 ± 4.5
HBP08-Ala8	GYHYERWAH	1.9 ± 0.6
HBP08-Ala9	GYHYERWIA	> 80
Pentapept-1	GYHYE	No-binding*
Pentapept-2	ERWIH	160 ± 80
HBP08-RI	d-HIWREYHYG	14.0 ± 4.5

* No binding was detected in the explored concentration range.
# Not determined due to poor solubility in PBS

The results of these experiments indicated that HBP08-Ala3, HBP08-Ala6, HBP08-Ala7, and HBP08-Ala9 are key for the binding, suggesting that the length of the peptide could be reduced. Therefore, we also tested the affinity of two peptides formed by the first (pentapept-1) or the last (pentapept-2) five residues of HBP08. In agreement with the data from alanine scanning, no binding was observed for the pentapep-1 in the range of concentration applied to the analysis of the other peptides. Differently, a K_d of 160 ± 80 μM was determined for pentapept-2, confirming the importance of the C-terminal end for the binding, but also indicating that the role of the residues at the N-terminal end is not negligible.

In analogy with previous investigations on the binding of proteins[7] or small molecules to HMGB1,[21, 36] we performed NMR Chemical Shift Perturbation (CSP) experiments (Figure 6B-D) to further characterize the interaction between HBP08 and both HMGB1-BoxA and BoxB. This analysis enabled us to identify the protein residues involved in the peptide binding (Table 3). These data were used to generate models of the complexes by computational docking with

Haddock.[37] In particular, the contacts suggested by CSP experiments were used as restraints during the docking procedure. Finally, the poses with the best Haddock score and the best correlation between predicted and experimentally determined affinities were selected for analysis. For both BoxA and BoxB the best correlation between the experimental and predicted affinities is ~ 0.6. The reasons of this rather low values can be related to both the approximation used for the computation of the binding affinity and inaccuracies of the models. However, similar values were also obtained using more accurate methods (MM-PBSA and Free Energy Perturbation).[38]

The analysis of the structures of the HBP08/BoxA and HPB08/BoxB complexes (Figure 6A and 6C) provides interesting clues about the specific interactions that drive the formation of the complexes. In fact, when in complex with BoxA, HBP08-His3 interacts with Asp66, HBP08-Trp7 is in contact with Arg23, Ser34, and Val35, and HBP08-His9 that MST experiments indicated as the more important residue for the formation of the complex occupies a small cavity delimited by Tyr15, Phe17 and Gln20. When in the complex with BoxB, HBP08-Tyr4 forms an h-bond interaction with the backbone of Arg96, HPB08-Trp7 is in contact with the aromatic rings of Phe101 and Trp132, and HBP08-His9 interacts with Ser106 with an h-bond.

We compared the structure of the HBP08/BoxA complex with the one of the CXCL12/BoxA complex, obtained in previous NMR investigations[7] [14] (Figure 6E). Of note, this analysis confirmed that the binding site of HBP08 or CXCL12 to BoxA shares residues and, therefore confirms the ability of the peptide to interfere with the formation of the CXCL12/HMGB1 heterocomplex.

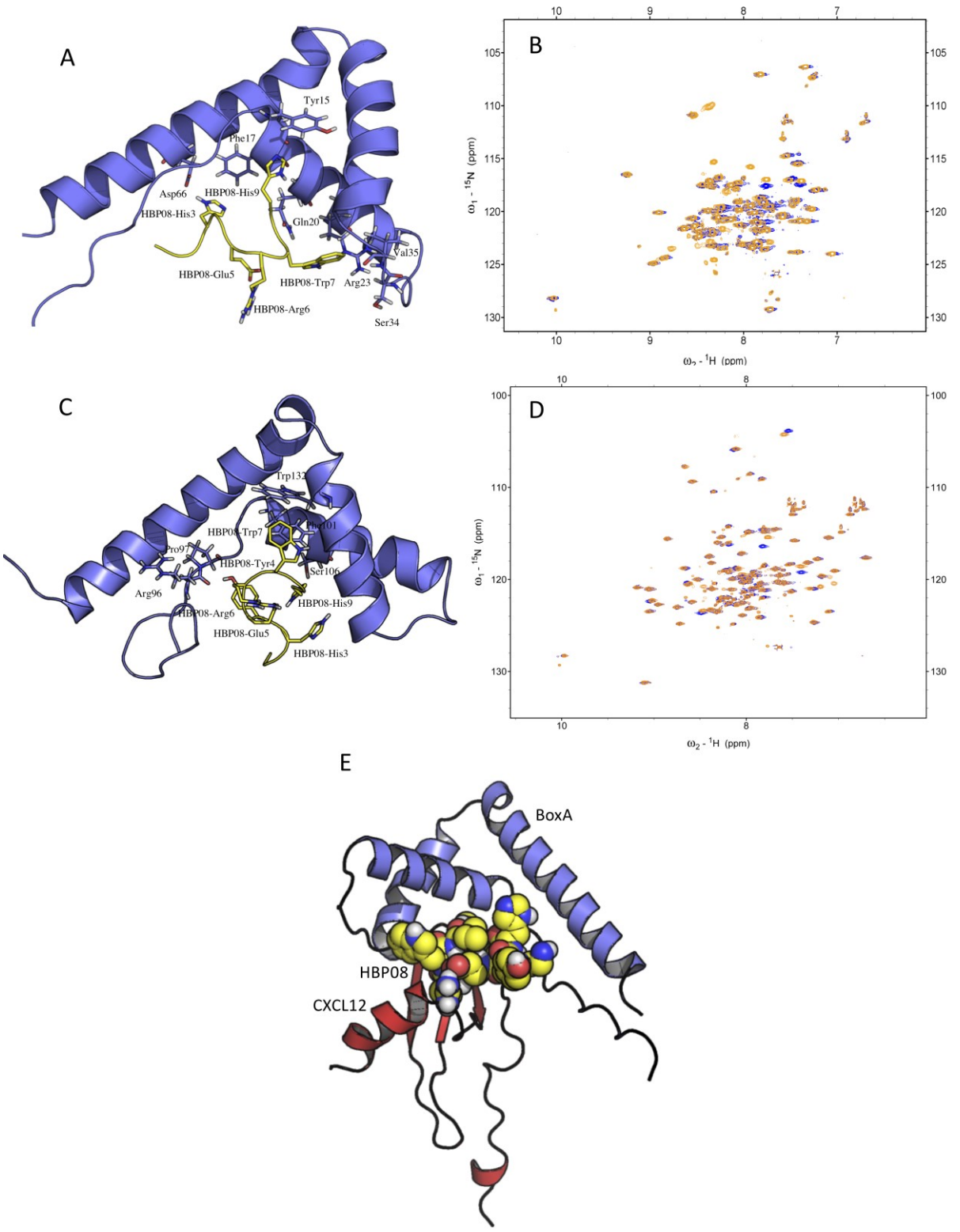

Figure 6. (A) Molecular model of the HBP08-BoxA complex. BoxA and HBP08 are represented as violet or yellow cartoons, respectively. The residues more important for the binding are represented as sticks colored by atom type. (**B**) NMR sprectra of BoxA alone (blue)

and in complex with HBP08 (orange). (**C**) Molecular model of the HBP08-BoxB complex. BoxA and HBP08 are represented as violet or yellow cartoons, respectively. The residues more important for the binding are represented as sticks colored by atom type. (**D**) NMR sprectra of BoxB alone (blue) and in complex with HBP08 (orange). (**E**) Comparison between the HBP08 binding mode and the structure of CXCL12-BoxA complex obtained by docking in our previous study [14].

Table 3. Residues Showing Significant Chemical-Shift Difference upon the HBP08 binding.

HMGB1 domain	Residues
BoxA	Y15, F17, V19, Q20, E25, K27, K28, K29, H30, S34, V35, E46
BoxB	D90, K95, A100, K113, G114, E115, G118, L119, D123, A125, G129, E130, M131, W132, N133

HBP08 retro-inverso

L-peptides are susceptible to the action of proteolytic enzymes such as peptidases, hindering their application *in vivo*. D-peptides are less prone to the action of peptidases and to the acidic hydrolysis that occurs in the stomach, which increases their oral bioavailability and half-live in the blood circulation. Furthermore, D-peptides have a lower immunogenicity.[39] Taken together, all these features make D-peptides suitable for drug development.[40]

To exploit the potential of D-peptides, we investigated the binding of a retro-inverso analog of HBP08 (HBP08-RI) made by D-amino acids in reversed order. The results of the binding experiments indicated that HBP08-RI has a lower but still good affinity for HMGB1 (K_d = 14.0 ± 4.5 μM), therefore representing a good candidate for future drug development studies.

Conclusions

The results presented here, show that HBP08is the first potent peptide inhibitors of the CXCL12/HMGB1 heterocomplex.

We and others have demonstrated, in the last decade, the relevance of this heterocomplex both in physiological and in pathological processes, and recently its crucial role in the perpetuation of the chronic inflammation observed in RA.[13] The lack of full remission in a portion of RA patients, and the evidence that the composition of the synovial tissue correlates with the response to the available treatments, calls for the identification of novel targets and the development of selective therapies.[17, 18] Therefore, small molecules or peptides able to hinder the formation of this heterocomplex could be useful as novel personalized therapeutic strategies.

The rational for designing a peptide targeting the formation of the CXCL12/HMGB1 heterocomplex, rather than targeting the CXCR4 receptor, stands in preserving the physiological functions of CXCR4, while inhibiting the detrimental effects exerted by the heterocomplex.

Multiple attempts have been made to identify small molecules able to bind HMGB1.[22] However, the majority of inhibitors reported in literature so far show a weak affinity for HMGB1 and a poor selectivity in targeting its synergistic interaction with CXCL12.[19] Recently, diflunisal has been reported as a specific inhibitor of the CXCL12/HMGB1 heterocomplex activity, without affecting TLR4 signaling. However, its Kd for HMGB1 in the mM range suggests that the biological effect, observed at a nano-molar concentration, could be the result of multi-target interactions.[21]

Out of the 13 candidates selected with the computational procedure, HBP08 resulted to be able to efficiently inhibit the synergy induced by the heterocomplex on murine cells transfected with the human CXCR4 and on human monocytes.

Previous studies of Al-Abed and coworkers[41] indicated that the TLR4 activation by HMGB1 can be inhibited by both BoxA and an anti-HMGB1 antibody (2G7) that interacts with HMGB1 binding to the region within the residues 53-63 of BoxA.[42] These results indicated that the same region, far from those we identified for the HBP08 binding, should be responsible of the HMGB1/TLR4 interaction and in fact, we have demonstrated that the developed peptide does not influence the HMGB1 functions on TLR4.

While the use of peptides as therapeutics remains challenging, we believe that this peptide can be exploited for therapeutic intervention while being immediately useful as a tool for cell-biologists to further dissect the inflammatory pathways triggered by the CXCL12/HMGB1 heterocomplex. Moreover, our biophysical and structural biology studies indicated the C-terminal end of the peptide as the most important for the interaction with both BoxA and BoxB, providing important information for the design of novel peptide-mimetic anti-inflammatory drugs.

Experimental section

Glycyrrhizin docking to HMGB1. A model of the HMGB1-glycyrrhizin complex was built by ligand docking, starting from NMR HMGB1 structure available in the protein data bank with the code 2YRQ. All the docking calculation were carried out using Glide (Schrodinger Inc.) in the version 2016-4.[43] The grid necessary to perform docking was centered in the COG (center of geometry) of the protein and both the enclosing and the bounding box were set bigger than entire protein, to allow a blind-docking, i.e. docking without previous knowledge of a binding site. Standard precision (SP) mode was used to score the resulting ligand-protein complexes. The twenty poses with the best Glide score were kept for further investigation. Finally, the structure with the best agreement with NMR CSP data by Mollica et al.[19] was selected as the most likely representative model of the HMGB1-glycyrrhizin complex.

Computational design of binding peptides. Peptides were designed following a multistep process. First, the model of the BoxA-glycyrrhizin complex was used to define the target binding site for the peptides. To this end, we selected all amino acids from BoxA for which at least a carbon atom was at a distance smaller than 7.5 Å from a glycyrrhizin carbon atom. These gave a list of 17 amino acids, namely: LYS_12, MET_13, SER_14, SER_15, TYR_16, ALA_17, VAL_20, GLU_21, ARG_24, GLU_25, LYS_28, SER_35, VAL_36, ASN_37, PHE_38, PHE_41, SER_42.

Since the size of glycyrrhizin is approximatively equal to the length of a linear 9-residue peptide we proceeded with the generation of 40,000 9-residue peptides with a random sequence. All these peptides were then docked on the BoxA domain using the torsional angular molecular dynamics (TMD) module[44, 45] of the software package ALMOST.[46]

The docking of the peptides was guided by a set of 17 synthetic NMR-like ambiguous upper-distance restraints[47] between the Cα atoms, i, of the residues of the binding site of BoxA and the Cα atoms, j, of the peptide,

$E^i_{pept} = \begin{cases} (d^i_{amb} - d_0)^2, if\ d^i_{amb} > d_0 \\ 0, if\ d^i_{amb} \leq d_0 \end{cases}$, where $d^i_{amb} = \left(\sum_{j \epsilon C\alpha\ pept} d_{ij}^{-6}\right)^{-1/6}$ and $d_0 = 7.5$ Å.

For each peptide, the structure with the smallest distance restraint violations among the 25 generated was then selected and minimized with the CHARMM 19 SASA implicit solvation force field.[48] All peptides were then ranked according to their binding energy, $\Delta E = E_{complex} - (E_{BoxA} + E_{pept})$, and the best 100 among the 40,000 generated were selected for the further analysis.

Peptide re-docking with Glide. The ability of the 100 peptides with the best CHARMM binding energy to form complexes with the BoxA domain of HMGB1 was then additionally assessed with the peptide-docking protocol of Glide,[49] implemented in the Schrodinger suite for molecular modeling (Version 2016-4).

Aiming to leave the algorithm free to explore the entire surface of the protein we performed, also in this case, blind docking using a grid positioned in the center of geometry (COG) and large enough to contain the entire BoxA.

For each peptide, the 15 best poses were saved for further analysis, resulting in a total of 1,500 peptide-BoxA complexes. The 200 complexes with the best Glide score were inspected and, for each peptide, only the best pose conserving the key glycyrrhizin interactions (i.e. Q20 and with R23) and binding mode in the region at the junction of the two arms of L-shape that characterize the two HMGB1 boxes was kept. Peptides without a glycyrrhizin-like pose in the

top 200 solutions were discarded. At the end of this process, 43 peptides were discarded and 57 retained for subsequent analysis.

Molecular dynamics (MD) and binding free energy calculations. To further assess the stability of the 57 selected complexes and to better estimate their affinity, we performed 0.5 μs MD simulations in explicit water using AMBER16. Snapshots from the corresponding trajectories were extracted to compute the binding energy ΔG with MM-GBSA, a computational method already applied in similar studies with positive results.[34, 50, 51]

All the peptide-BoxA complexes were solvated in a water box with a minimum distance from the protein surface of 10 Å. The total charge of the system was neutralized adding a proper number of Cl^-/Na^+ ions.

All molecular dynamics simulations were carried out using the ff14SB[52] force field for the protein, the TIP3P model[53] for water, and the parameters proposed by Joung et al.[54] for the counter-ions. The peptide-BoxA complexes were first relaxed with a two-step computational protocol consisting of energy minimization for 10,000 steps or until the energy gradient of 0.2 kcal/mol/Å^2 was reached, restraining the backbone atomic coordinates with a harmonic restraint (k = 20 kcal/mol/Å^2), followed by an unrestrained energy minimization for 100,000 steps (or until an energy gradient of 0.0001 kcal/mol/Å^2 was reached). The systems were then heated to their final temperature of 300K in 40 ps. All simulations were run at constant volume, restraining the backbone coordinates (k = 20 kcal/mol/Å^2) during the first 20 ps. Subsequently, the velocities were assigned again, and the systems equilibrated for 20ps at constant pressure (1 Atm). Finally, all complexes were simulated for 500 ns. All the simulations were analyzed and only those in which the peptide –BoxA complex was stable, were retained for MM-GBSA analysis. 500 snapshots selected in the more stable part of the simulation were used in the MM-GBSA calculations. Water molecules and counter-ions were stripped, while the protein and the peptide were parametrized using the same force field as in MD simulations. The polar

contribution to solvation energy was computed with the Onufriev, Bashford and Case model setting the dielectric constant to 1 for the solute and 80 for the solvent.[55] Finally, the 13 peptides (Table 1) with the best free energy ΔG were purchased and tested experimentally *in vitro*.

Proteins and peptides. CXCL12 was chemically synthesized as previously.[56] Histidine tagged HMGB1, BoxA and BoxB, with or without 15N-labeled labeling, were expressed at the Institute of Research in Biomedicine Protein Facility (Bellinzona, Switzerland) as previously described,[12] and stored in phosphate-buffered saline (PBS; D8537, Sigma Aldrich, Saint Louis, MO, USA). All the peptides were custom-synthesized and HPLC-purified by GenScript (New Jersey, USA). Peptides were reconstituted with DMSO and stored at -20 ºC. HPLC-MS was used to confirm 98% or higher purity for each peptide.

Cells. A murine 300.19 PreB cell line stably transfected with the human CXCR4 was kept in culture in RPMI-1640, supplemented with 10% Fetal Bovine Serum, 1x non-essential amino acids, 1 mM sodium pyruvate, 20 mM GlutaMAX, 50 µM β-Mercaptoethanol, 50 U/ml Penicillin and 50 µg/ml Streptomycin (GIBCO). Human monocytes were freshly isolated from buffy-coats obtained from a spontaneous donation from healthy individuals (Schweizerisches Rotes Kreuz, Basel), using positive selection with CD14 microbeads (Miltenyi Biotec), as previously described.[7]

Chemotaxis assay. Chemotaxis was performed using Boyden chambers with 5µm pore membranes, as previously described.[57] Murine 300.19 PreB cells stably transfected with the human CXCR4, or freshly isolated human monocytes were allowed to migrate for 90 min at 37°C in response to a sub-optimal CXCL12 concentration (1 nM), in the presence or absence of HMGB1 (300 nM), as previously described.[7] Inhibition of the synergistic activity of the CXCL12/HMGB1 heterocomplex was obtained by incubating CXCL12 and HMGB1 with 200 µM glycyrrhizin (Sigma Aldrich), as positive control.[7] All peptides, at 100 µM, were

incubated with CXCL12 and HMGB1 before assessing chemotaxis, to evaluate their ability to interfere with the heterocomplex formation and inhibit the synergistic effect of HMGB1.

Assessment of peptides toxicity. Peptides' toxicity was assessed on the murine 300.19 PreB cell line expressing the human CXCR4, and on human monocytes. Cells were incubated for 2h in the presence of the different peptides at 100 μM, stained by AnnexinVFITC/Propidium Iodide following manufacturer's instructions, and cell viability was analyzed by flow cytometry in comparison to the untreated control.

Cytokines quantification. Human monocytes were incubated for 8h at 37°C at a density of $1x10^6$ cell/ml in RPMI-1640 supplemented with 0.05% pasteurized human albumin in the presence or absence of 20nM HMGB1. A polyclonal neutralizing antibody against TLR4 (AF1478, R&D System,) was used to block TLR4 engagement. HBP08 at 100 μM was tested for its ability to inhibit HMGB1/TLR4-mediated release of cytokines. Quantification of IL1β, IL6, IL8, IL10, IL12, and TNF in the supernatants was determined by using Cytometric Bead Array (CBA) - Human Inflammatory Cytokines Kit (551811, BD Biosciences, San Jose, CA, USA), that allows the determination of the indicated human cytokines simultaneously. Acquisition was performed with FACSCanto II (BD Biosciences, San Jose, CA), and the concentration was calculated from the MFI according to a standard curve of each cytokine.

Affinity determination by Microscale thermophoresis (MST). The binding affinity (K_d) between the target proteins (6His-tagged-HMGB1, 6His-tagged-BoxA and 6His-tagged-BoxB) and HBP08 peptide were measured by microscale thermophoresis (MST).[58]

Briefly, histidine tagged target proteins were labeled by a His-tag specific dye (Monolith His-Tag Labeling Kit RED-tris-NTA (MO-L008)), NanoTemper® Technologies GmbH, München, Germany), for 30 minutes at room temperature. A fixed concentration of the labeled target protein (HMGB1, BoxA or BoxB) was mixed with 16 1:1 serial dilution of the HBP08

peptide (range 0.5mM-20 nM). The protein and the peptide were incubated for 15 minutes at room temperature. MST analysis was performed using premium-coated capillaries on a NanoTemper instrument, using the following experimental settings: LED power of 5% (for fluorescence excitation), and laser power 40% (to create temperature gradient). K_d values were calculated from compound concentration-dependent changes in normalized fluorescence (Fnorm).

In all the experiments both protein and peptides were dissolvent in Dulbecco's Phosphate Buffered Saline (PBS; D8537, Sigma Aldrich, Saint Louis, MO, USA).

At least two independent experiments were performed to compute the K_d values. Data were analyzed with the NanoTemper analysis software and the fitting performed by using the K_d model as implemented in the MO.Affinity.Analysis software (v. 2.3).

Chemical Shift perturbation NMR experiments. Spectra were recorded on a Bruker Avance 600 MHz NMR spectrometer at 298 K, pH 6 in 20mM sodium phosphate, and 20mM NaCl buffer at a protein concentration of 390 μM. In mapping experiments, HMGB1-BoxA and HMGB1-BoxB were uniformly labeled with ^{15}N while the peptide HBP08 was unlabelled. Chemical shift assignment was based on published data (BMRB entry 11532).[59] Briefly, overlay of [^{15}N,^{1}H]-HSQC spectra of free or HMGB1-BoxA and in complex with unlabelled peptide at 1:10 ratio allowed identification of HMGB1-BoxA residues for which the associated NMR signal changed upon complex formation, indicating alterations in their local chemical environment. The NMR data were analyzed with NMRFAM-SPARKY software.[60] NMR mapping was performed as previously described.[61, 62] Briefly, overlay of 15N-HSQC spectra of labeled BoxA or BoxB free or bound to the peptide allowed identification residues whose NMR signal

changed upon complex formation, indicating that they were affected by peptide binding. Changes were identified by manual inspection

and by the CSP = $((\Delta\delta_H)^2+(\Delta\delta_N/10)^2)^{1/2}$

Generation of structural models of the HBP08/BoxA and HBP08/BoxB complex. Chemical shift perturbation data were used to generate a model of both *HBP08-BoxA and HBP08-BoxB* complexes by docking calculations. In analogy with previous studies on HMGB1,[19, 21] the calculations were performed using the Haddock v2.4 program in the webserver implementation.[37, 63] 5000 structures were generated in the first step and the best 400 were retained after a semi-flexible optimization and refinement with a short simulation run in explicit water.. The structures were clustered by the Fraction of Common Contacts Clustering (FCC) clustering algorithm with a cut-off value of 0.6. During the docking, the residues Tyr15, Phe17, Val19, Lys27, Lys28 Ser34 and Val35 of BoxA, Asp90, Lys95, Ala100, Lys113, Asp123, Ala125, Gly129 of BoxB and Asn133 as well as His3, Trp7 and His9 of HBP08 were considered as active, while no passive residues were defined. Residues influenced by HBP08 binding, but buried inside the protein structure or outside of the L-shape binding site identified for both CXCL12 and glycyrrhizin were not considered in the definition of the ambiguous restraints. Only HBP08 was considered fully flexible during the simulations. All the other parameters were left at their default values.

Finally, the Prodigy program[64], was used to perform an virtual alanine scanning, using of the first 12 complexes (ranked by Haddock score) with BoxA and BoxB, respectively. Results were then compared with those obtained by MST (Table 2 and Table S2 and S3). Starting from the cluster with the best Haddock score, the pose associated with the best correlation with the measured affinities was selected as representative structure.

Statistical analysis. The statistical significance between more than two groups was calculated by using one-way ANOVA followed by Dunnett's multicomparisons test or two-way ANOVA

followed by Tukey's multicomparisons test, as appropriate. A p-value below 0.05 was considered as significant.

Ancillary information

Supporting Information

Molecular Formula Strings (CSV). Structures of the HBP08/BoxA and HBP08/BoxB (PDB). Results of the affinity prediction, performed by MM-GBSA, for the 57 peptides selected after docking calculations. Results of the alanine scanning calculations on the best docking solution produced by Haddock for the BoxA/HBP08 and BoxB/HBP08 complex. Representation of docking structures between Box-A of HMGB1 and tested peptides. Assessment of cell viability on preB 300.19 cells and human monocytes. MST binding curves for the binding of HBP08 to BoxA and BoxB.

Conflict of interests

A.C., M.U. and J.S. submitted a patent application entitled "PEPTIDE INHIBITORS TARGETING THE CXCL12/HMGB1 INTERACTION AND USES THEREOF", application number PCT/EP2019/057125, filing date 21 March 2019, status: pending

Corresponding authors:

Dr. Andrea Cavalli
Institute for Research in Biomedicine
Università della Svizzera italiana
Via Vincenzo Vela 6
CH-6500 Bellinzona, Switzerland
Email: andrea.cavalli@irb.usi.ch

Dr. Mariagrazia Uguccioni
Institute for Research in Biomedicine
Università della Svizzera italiana
Via Vincenzo Vela 6
CH-6500 Bellinzona, Switzerland
Email: mariagrazia.uguccioni@irb.usi.ch

Author contributions

J.S. designed, performed and analyzed the computer simulations and MST experiments, wrote the manuscript. V.C. designed the *in vitro* experiments, performed chemotaxis, assessed the toxicity of the peptides and their activity on TLR4, wrote the manuscript. E.M.A.F. performed and analyzed the simulations. G.D.A. performed chemotaxis experiments and assessed the toxicity of the peptides. M.G. performed MST experiments. G.D. performed chemotaxis experiments. G.G. contributed to the computational design and MST experiments. L.S and L.V. analyzed NMR experiments. M.P. expressed and purified recombinant proteins. M.U. designed the experiments and supervised the work, wrote the manuscript. A.C. designed the computational pipeline and supervised the work, performed simulations, wrote the code for initial peptide docking, wrote the manuscript. All the authors discussed and reviewed the manuscript.

Abbreviations used

CSP: Chemical Shift Perturbation; GPCR: G-protein-coupled receptors;HMGB1: High Mobility Group Box1; IL: Interleukin; MM-GBSA: Molecular Mechanics-Generalized Born Surface Area; MM-GBSA: Molecular Mechanics-Poisson Boltzmann Surface Area; MD: Molecular Dynamics; NF-kB: Nuclear Factor kappa-B (NF-kB); NMR: Nuclear Magnetic Resonance; RA: Rheumatoid Arthritis;RAGE: Receptor for advanced glycation endproducts;TLR4: Toll-Like Receptor 4 (TLR4); TNF: Tumor Necrosis Factor

Acknowledgments

The authors thank Dr. Laurent Perez from the IRB protein facility for the synthesis of HMGB1. This study was supported by the Swiss National Science Foundation (3100A0-143718/1 to M.U. and 31003A-166472 to A.C.). M.U. has received funding for this project from the European Union's Programs for research, technological development and demonstration under grant agreements ADITEC – 280873 (FP7), and TIMER – 281608 (FP7). Further supports were given by the San Salvatore Foundation, the Novartis Foundation, the Gottfried and Julia Bangerter-Rhyner-Foundation, and the Helmut Horten Foundation. A.C. has received founding for this project from the Swiss Cancer League (KLS-3839-02-2016-R).

References

1. Charo, I. F.; Ransohoff, R. M., The many roles of chemokines and chemokine receptors in inflammation. *N. engl. j. med.* 2006, *354*, 610-621.
2. Muller, C. E.; Schiedel, A. C.; Baqi, Y., Allosteric modulators of rhodopsin-like G protein-coupled receptors: opportunities in drug development. *Pharmacol. ther* 2012, *135*, 292-315.
3. Wells, T. N.; Power, C. A.; Shaw, J. P.; Proudfoot, A. E., Chemokine blockers--therapeutics in the making? *Trends pharmacol. sci.* 2006, *27*, 41-47.
4. Griffith, J. W.; Sokol, C. L.; Luster, A. D., Chemokines and chemokine receptors: positioning cells for host defense and immunity. *Annu. rev. immunol.* 2014, *32*, 659-702.
5. Cecchinato, V.; D'Agostino, G.; Raeli, L.; Uguccioni, M., Chemokine interaction with synergy-inducing molecules: fine tuning modulation of cell trafficking. *J. leukoc. biol.* 2016, *99* , 851-855.
6. Proudfoot, A. E.; Uguccioni, M., Modulation of Chemokine Responses: Synergy and Cooperativity. *Front. immunol.* 2016, *7*, 183.
7. Schiraldi, M.; Raucci, A.; Munoz, L. M.; Livoti, E.; Celona, B.; Venereau, E.; Apuzzo, T.; De Marchis, F.; Pedotti, M.; Bachi, A.; Thelen, M.; Varani, L.; Mellado, M.; Proudfoot, A.; Bianchi, M. E.; Uguccioni, M., HMGB1 promotes recruitment of inflammatory cells to damaged tissues by forming a complex with CXCL12 and signaling via CXCR4. *J. exp med* 2012, *209*, 551-563.
8. Van Der Poll, T.; Wiersinga, W. J., 47 - Sepsis. In *Infectious diseases (Fourth Edition)*, Cohen, J.; Powderly, W. G.; Opal, S. M., Eds. Elsevier: 2017, 415-426.
9. Lotze, M. T.; Tracey, K. J., High-mobility group box 1 protein (HMGB1): nuclear weapon in the immune arsenal. *Nat. rev immunol.* 2005, *5*, 331-342.
10. Andersson, U.; Tracey, K. J., HMGB1 is a therapeutic target for sterile inflammation and infection. *Annu rev. immunol.* 2011, *29*, 139-162.

11. Yang, H.; Antoine, D. J.; Andersson, U.; Tracey, K. J., The many faces of HMGB1: molecular structure-functional activity in inflammation, apoptosis, and chemotaxis. *J. leukoc. biol.* 2013, *93*, 865-873.
12. Venereau, E.; Casalgrandi, M.; Schiraldi, M.; Antoine, D. J.; Cattaneo, A.; De Marchis, F.; Liu, J.; Antonelli, A.; Preti, A.; Raeli, L.; Shams, S. S.; Yang, H.; Varani, L.; Andersson, U.; Tracey, K. J.; Bachi, A.; Uguccioni, M.; Bianchi, M. E., Mutually exclusive redox forms of HMGB1 promote cell recruitment or proinflammatory cytokine release. *J. exp. med.* 2012, *209*, 1519-1528.
13. Cecchinato, V.; D'Agostino, G.; Raeli, L.; Nerviani, A.; Schiraldi, M.; Danelon, G.; Manzo, A.; Thelen, M.; Ciurea, A.; Bianchi, M. E.; Rubartelli, A.; Pitzalis, C.; Uguccioni, M., Redox-Mediated Mechanisms Fuel Monocyte Responses to CXCL12/HMGB1 in Active Rheumatoid Arthritis. *Front. immunol.* 2018, *9*, 2118..
14. Fassi, E. M. A.; Sgrignani, J.; D'Agostino, G.; Cecchinato, V.; Garofalo, M.; Grazioso, G.; Uguccioni, M.; Cavalli, A., Oxidation State Dependent Conformational Changes of HMGB1 Regulate the Formation of the CXCL12/HMGB1 Heterocomplex. *Comput. struct. biotechnol. J.* 2019, *17*, 886-894.
15. Vénéreau, E.; Ceriotti, C.; Bianchi, M. E., DAMPs from Cell Death to New Life. *Front. immunol.* 2015, *6*, 422.
16. Yang, H.; Wang, H.; Ju, Z.; Ragab, A. A.; Lundback, P.; Long, W.; Valdes-Ferrer, S. I.; He, M.; Pribis, J. P.; Li, J.; Lu, B.; Gero, D.; Szabo, C.; Antoine, D. J.; Harris, H. E.; Golenbock, D. T.; Meng, J.; Roth, J.; Chavan, S. S.; Andersson, U.; Billiar, T. R.; Tracey, K. J.; Al-Abed, Y., MD-2 is required for disulfide HMGB1-dependent TLR4 signaling. *J. exp. med.* 2015, *212*, 5-14.
17. Pitzalis, C.; Kelly, S.; Humby, F., New learnings on the pathophysiology of RA from synovial biopsies. *Curr. opin. rheumat.* 2013, *25*, 334-344.
18. Smolen, J. S.; Aletaha, D.; Barton, A.; Burmester, G. R.; Emery, P.; Firestein, G. S.; Kavanaugh, A.; McInnes, I. B.; Solomon, D. H.; Strand, V.; Yamamoto, K., Rheumatoid arthritis. *Nat. rev. dis. primers* 2018, *4*, 18001.
19. Mollica, L.; De Marchis, F.; Spitaleri, A.; Dallacosta, C.; Pennacchini, D.; Zamai, M.; Agresti, A.; Trisciuoglio, L.; Musco, G.; Bianchi, M. E., Glycyrrhizin binds to high-mobility group box 1 protein and inhibits its cytokine activities. *Chem Biol* 2007, *14*, 431-441.
20. Choi, H. W.; Tian, M.; Song, F.; Venereau, E.; Preti, A.; Park, S. W.; Hamilton, K.; Swapna, G. V.; Manohar, M.; Moreau, M.; Agresti, A.; Gorzanelli, A.; De Marchis, F.; Wang, H.; Antonyak, M.; Micikas, R. J.; Gentile, D. R.; Cerione, R. A.; Schroeder, F. C.; Montelione, G. T.; Bianchi, M. E.; Klessig, D. F., Aspirin's Active Metabolite Salicylic Acid Targets High Mobility Group Box 1 to Modulate Inflammatory Responses. *Mol. med.* 2015, *21*, 526-535.
21. De Leo, F.; Quilici, G.; Tirone, M.; De Marchis, F.; Mannella, V.; Zucchelli, C.; Preti, A.; Gori, A.; Casalgrandi, M.; Mezzapelle, R.; Bianchi, M. E.; Musco, G., Diflunisal targets the HMGB1/CXCL12 heterocomplex and blocks immune cell recruitment. *EMBO rep.* *20*, e47788.
22. VanPatten, S.; Al-Abed, Y., High Mobility Group Box-1 (HMGb1): Current Wisdom and Advancement as a Potential Drug Target. *J. med. chem.* 2018, *61*, 5093-5107.
23. Henninot, A.; Collins, J. C.; Nuss, J. M., The Current State of Peptide Drug Discovery: Back to the Future? *J. med. chem.* 2018, *61*, 1382-1414.
24. Petta, I.; Lievens, S.; Libert, C.; Tavernier, J.; De Bosscher, K., Modulation of Protein-Protein Interactions for the Development of Novel Therapeutics. *Mol. ther.* 2016, *24*, 707-718.
25. Bruzzoni-Giovanelli, H.; Alezra, V.; Wolff, N.; Dong, C. Z.; Tuffery, P.; Rebollo, A., Interfering peptides targeting protein-protein interactions: the next generation of drugs? *Drug disc. today* 2018, *23*, 272-285.

26. Rader, A. F. B.; Weinmuller, M.; Reichart, F.; Schumacher-Klinger, A.; Merzbach, S.; Gilon, C.; Hoffman, A.; Kessler, H., Orally Active Peptides: Is There a Magic Bullet? *Angew. chem. int. ed.* 2018, *57*, 14414-14438.
27. Michaeli, A.; Mezan, S.; Kuhbacher, A.; Finkelmeier, D.; Elias, M.; Zatsepin, M.; Reed, S. G.; Duthie, M. S.; Rupp, S.; Lerner, I.; Burger-Kentischer, A., Computationally Designed Bispecific MD2/CD14 Binding Peptides Show TLR4 Agonist Activity. *J. immunol* 2018, *201*, 3383-3391.
28. Lee, A. C.; Harris, J. L.; Khanna, K. K.; Hong, J. H., A Comprehensive Review on Current Advances in Peptide Drug Development and Design. *Int. j. mol. sci.* 2019, *20*, 2383.
29. Lau, J. L.; Dunn, M. K., Therapeutic peptides: Historical perspectives, current development trends, and future directions. *Bioorg. med. chem.* 2018, *26*, 2700-2707.
30. Tubert-Brohman, I.; Sherman, W.; Repasky, M.; Beuming, T., Improved docking of polypeptides with Glide. *J. chem. inf. model.* 2013, *53*, 1689-1699.
31. Rastelli, G.; Del Rio, A.; Degliesposti, G.; Sgobba, M., Fast and accurate predictions of binding free energies using MM-PBSA and MM-GBSA. *J. comput. chem.* 2010, *31*, 797-810.
32. Grazioso, G.; Pome, D. Y.; Matera, C.; Frigerio, F.; Pucci, L.; Gotti, C.; Dallanoce, C.; De Amici, M., Design of novel alpha7-subtype-preferring nicotinic acetylcholine receptor agonists: application of docking and MM-PBSA computational approaches, synthetic and pharmacological studies. *Bioorg. med. chem. lett.* 2009, *19*, 6353-6357.
33. Geng, L.; Wang, Z.; Yang, X.; Li, D.; Lian, W.; Xiang, Z.; Wang, W.; Bu, X.; Lai, W.; Hu, Z.; Fang, Q., Structure-based Design of Peptides with High Affinity and Specificity to HER2 Positive Tumors. *Theranostics* 2015, *5*, 1154-1165.
34. Lammi, C.; Sgrignani, J.; Roda, G.; Arnoldi, A.; Grazioso, G., Inhibition of PCSK9(D374Y)/LDLR Protein-Protein Interaction by Computationally Designed T9 Lupin Peptide. *ACS med. chem. lett.* 2019, *10*, 425-430.
35. Garofalo, M.; Grazioso, G.; Cavalli, A.; Sgrignani, J., How Computational Chemistry and Drug Delivery Techniques Can Support the Development of New Anticancer Drugs. *Molecules* 2020, *25*, 1756.
36. De Leo, F.; Quilici, G.; De Marchis, F.; Mantonico, M. V.; Bianchi, M. E.; Musco, G., Discovery of 5,5'-Methylenedi-2,3-Cresotic Acid as a Potent Inhibitor of the Chemotactic Activity of the HMGB1·CXCL12 Heterocomplex Using Virtual Screening and NMR Validation. *Front. chem.* 2020, *8*, 598710.
37. Dominguez, C.; Boelens, R.; Bonvin, A. M. J. J., HADDOCK: A Protein−Protein Docking Approach Based on Biochemical or Biophysical Information. *J. am. chem. soc.* 2003, *125*, 1731-1737.
38. Steinbrecher, T. B.; Dahlgren, M.; Cappel, D.; Lin, T.; Wang, L.; Krilov, G.; Abel, R.; Friesner, R.; Sherman, W., Accurate Binding Free Energy Predictions in Fragment Optimization. *J. chem. inf. mod.* 2015, *55*, 2411-2420.
39. Arranz-Gibert, P.; Ciudad, S.; Seco, J.; García, J.; Giralt, E.; Teixidó, M., Immunosilencing peptides by stereochemical inversion and sequence reversal: retro-D-peptides. *Sci. rep.* 2018, *8*, 6446.
40. Liu, M.; Li, X.; Xie, Z.; Xie, C.; Zhan, C.; Hu, X.; Shen, Q.; Wei, X.; Su, B.; Wang, J.; Lu, W., D-Peptides as Recognition Molecules and Therapeutic Agents. *Chem. rec.* 2016, *16*, 1772-1786.
41. He, M.; Bianchi, M. E.; Coleman, T. R.; Tracey, K. J.; Al-Abed, Y., Exploring the biological functional mechanism of the HMGB1/TLR4/MD-2 complex by surface plasmon resonance. *Mol. med.* 2018, *24*, 21-30.
42. Qin, S.; Wang, H.; Yuan, R.; Li, H.; Ochani, M.; Ochani, K.; Rosas-Ballina, M.; Czura, C. J.; Huston, J. M.; Miller, E.; Lin, X.; Sherry, B.; Kumar, A.; Larosa, G.; Newman,

W.; Tracey, K. J.; Yang, H., Role of HMGB1 in apoptosis-mediated sepsis lethality. *J.exp. med.* 2006, *203*, 1637-42.
43. Friesner, R. A.; Banks, J. L.; Murphy, R. B.; Halgren, T. A.; Klicic, J. J.; Mainz, D. T.; Repasky, M. P.; Knoll, E. H.; Shelley, M.; Perry, J. K.; Shaw, D. E.; Francis, P.; Shenkin, P. S., Glide: a new approach for rapid, accurate docking and scoring. 1. Method and assessment of docking accuracy. *J. med. chem.* 2004, *47*, 1739-1749.
44. Stein, E. G.; Rice, L. M.; Brunger, A. T., Torsion-angle molecular dynamics as a new efficient tool for NMR structure calculation. *J magn. reson.* 1997, *124*, 154-164.
45. Guntert, P.; Mumenthaler, C.; Wuthrich, K., Torsion angle dynamics for NMR structure calculation with the new program DYANA. *J. mol. biol.* 1997, *273*, 283-298.
46. Fu, B.; Sahakyan, A. B.; Camilloni, C.; Tartaglia, G. G.; Paci, E.; Caflisch, A.; Vendruscolo, M.; Cavalli, A., ALMOST: an all atom molecular simulation toolkit for protein structure determination. *J. comput. chem.* 2014, *35*, 1101-1005.
47. Dominguez, C.; Boelens, R.; Bonvin, A. M., HADDOCK: a protein-protein docking approach based on biochemical or biophysical information. *J. am. chem. soc.* 2003, *125*, 1731-1737.
48. Ferrara, P.; Apostolakis, J.; Caflisch, A., Evaluation of a fast implicit solvent model for molecular dynamics simulations. *Proteins* 2002, *46*, 24-33.
49. Celie, P. H. N.; Klaassen, R. V.; van Rossum-Fikkert, S. E.; van Elk, R.; van Nierop, P.; Smit, A. B.; Sixma, T. K., Crystal structure of acetylcholine-binding protein from Bulinus truncatus reveals the conserved structural scaffold and sites of variation in nicotinic acetylcholine receptors. *J. biol. chem.* 2005, *280*, 26457-26466.
50. Lammi, C.; Zanoni, C.; Aiello, G.; Arnoldi, A.; Grazioso, G., Lupin Peptides Modulate the Protein-Protein Interaction of PCSK9 with the Low Density Lipoprotein Receptor in HepG2 Cells. *Sci. rep.* 2016, *6*, 29931.
51. Ylilauri, M.; Pentikainen, O. T., MMGBSA as a tool to understand the binding affinities of filamin-peptide interactions. *J. chem. inf. model.* 2013, *53* (10), 2626-33.
52. Maier, J. A.; Martinez, C.; Kasavajhala, K.; Wickstrom, L.; Hauser, K. E.; Simmerling, C., ff14SB: Improving the Accuracy of Protein Side Chain and Backbone Parameters from ff99SB. *J. chem. theory comput.* 2015, *11*, 3696-3713.
53. Jorgensen, W. L.; Chandrasekhar, J.; Madura, J. D.; Impey, R. W.; Klein, L. M., Comparison of simple potential functions for simulating liquid water. *J. chem. phys.* 1983, *79*, 926-935.
54. Joung, I. S.; Cheatham, T. E., Determination of alkali and halide monovalent ion parameters for use in explicitly solvated biomolecular simulations. *J. phys. chem. B* 2008, *112*, 9020-9041.
55. Onufriev, A.; Bashford, D.; Case, D. A., Exploring protein native states and large-scale conformational changes with a modified generalized born model. *Proteins* 2004, *55* (2), 383-94.
56. Clark-Lewis, I.; Vo, L.; Owen, P.; Anderson, J., Chemical synthesis, purification, and folding of C-X-C and C-C chemokines. *Meth. enzymol.* 1997, *287*, 233-250.
57. Uguccioni, M.; D'Apuzzo, M.; Loetscher, M.; Dewald, B.; Baggiolini, M., Actions of the chemotactic cytokines MCP-1, MCP-2, MCP-3, RANTES, MIP-1 alpha and MIP-1 beta on human monocytes. *Eur. j. immunol.* 1995, *25*, 64-68.
58. Jerabek-Willemsen, M.; Wienken, C. J.; Braun, D.; Baaske, P.; Duhr, S., Molecular interaction studies using microscale thermophoresis. *Assay drug dev. technol.* 2011, *9*, 342-353.
59. Hornemann, S.; von Schroetter, C.; Damberger, F. F.; Wuthrich, K., Prion protein-detergent micelle interactions studied by NMR in solution. *J. biol. chem.* 2009, *284*, 22713-22721.

60. Lee, W.; Tonelli, M.; Markley, J. L., NMRFAM-SPARKY: enhanced software for biomolecular NMR spectroscopy. *Bioinformatics* 2015, *31*, 1325-1327.
61. Bardelli, M.; Livoti, E.; Simonelli, L.; Pedotti, M.; Moraes, A.; Valente, A. P.; Varani, L., Epitope mapping by solution NMR spectroscopy. *J. mol. recognit.* 2015, *28*, 393-400.
62. Simonelli, L.; Beltramello, M.; Yudina, Z.; Macagno, A.; Calzolai, L.; Varani, L., Rapid structural characterization of human antibody-antigen complexes through experimentally validated computational docking. *J. mol. biol.* 2010, *396*, 1491-1507.
63. van Zundert, G. C. P.; Rodrigues, J.; Trellet, M.; Schmitz, C.; Kastritis, P. L.; Karaca, E.; Melquiond, A. S. J.; van Dijk, M.; de Vries, S. J.; Bonvin, A., The HADDOCK2.2 Web Server: User-Friendly Integrative Modeling of Biomolecular Complexes. *J. mol. biol.* 2016, *428*, 720-725.
64. Xue, L. C.; Rodrigues, J. P.; Kastritis, P. L.; Bonvin, A. M.; Vangone, A., PRODIGY: a web server for predicting the binding affinity of protein-protein complexes. *Bioinformatics* 2016, *32*, 3676-3678.

Table of Contents